16th World Conference on Earthquake, 16WCEE 2017
Santiago Chile, January 9th to 13th 2017
Paper N° 3242
Registration Code: S-S1461888728

SHEAR BEHAVIOR OF CONTINUOUS REINFORCED CONCRETE HAUNCHED BEAMS SUBJECTED TO CYCLIC LOADING

A. Tena-Colunga[(1)], L. A. Urbina-Californias[(2)], H. I. Archundia-Aranda[(3)]

[(1)] *Professor, Departamento de Materiales, Universidad Autónoma Metropolitana Azcapotzalco, email: atc@correo.azc.uam.mx*
[(2)] *Professor, Universidad Politécnica de Chimalhuacán, e-mail: ucla_1985@yahoo.com*
[(3)] *Professor, Departamento de Materiales, Universidad Autónoma Metropolitana Azcapotzalco, email: archundia@azc.uam.mx*

Abstract

Reinforced concrete haunched beams (RCHBs) are structural elements commonly used in buildings and bridges in Mexico and other countries worldwide. For example, in Mexico City there are several midrise buildings with RCHBs (old and recent). It is well known that the shear behavior of RCHBs is quite different from prismatic ones. Nevertheless, Mexican and United States codes do not include specific guides to design them.

Based upon previous experimental research studies based upon static and cyclic testing of simply-supported RCHBs deficient in shear, the authors have proposed accurate enough methods to design RCHBs in shear supported by: a) the section approach and, b) strut-and-tie (truss model) approach. However, it is also well known from theory that the contribution of the longitudinal inclined reinforcement of RCHBs in resisting shear is different for a simply supported condition with respect to a continuity condition. To the authors´ knowledge, there are no experimental data available about the cyclic behavior of RC haunched beams deficient in shear tested under a continuity condition.

Therefore, in this paper the research results and interpretations of the testing of four prototype continuous reinforced concrete beams (three haunched and one prismatic) designed to develop a shear failure under cyclic loading are presented. Subject beams were tested with minimum shear reinforcement. The studied haunched length is one-third the effective span of the beam. The considered angles of slope of haunch from horizontal vary from 0^0 (prismatic) to 8^0. Cyclic tests were displacement-controlled, and two cycles at the same displacement were set in the displacement history which considers a geometrical increment of target displacements.

The parameters under study with respect to the shear-resisting mechanism are: (a) the angle of haunch from horizontal and its impact on the concrete strength, (b) the contribution of the inclined longitudinal steel reinforcement and, (c) the contribution of the transverse steel reinforcement. Differences in the cyclic shear behavior of haunched beams with respect to prismatic beams were monitored. Previously proposed design equations were examined, and it was confirmed that these equations allows to reasonably assessing their shear strength for design purposes. The obtained results from the cyclic testing in continuity conditions allow one to corroborate what it was observed in previous testing for simply supported beams: reinforced concrete haunched beams are more efficient than reinforced concrete prismatic beams, even when they fail in shear.

Keywords: haunched beams, nonprismatic elements, shear strength, deformation capacity, cyclic testing

1. Introduction

Reinforced concrete haunched beams (RCHBs) are an attractive structural solution for buildings and bridges with large bay widths or spans. The use of RCHBs conceptually offers some structural and nonstructural advantages over prismatic beams. For example, a more efficient lateral stiffness or moment capacity to self-weight ratio is obtained using RCHBs rather than prismatic beams. Also, the use of RCHBs allow engineers to provide an smaller effective depth at midspan which eases the placement of different facilities in buildings (i.e., air conditioning, piping) and a higher clearance in bridges. However, their major disadvantage is that their use often involves higher construction costs, as special formwork and qualified construction workers are required.

RCHBs have been used in buildings and bridges worldwide for a long time. However, recent applications in the United States and Europe are mostly in bridges (Fig. 1), perhaps because of construction costs directed related to workmanship. New applications in buildings are mostly confined to countries where the manpower is much cheaper like Mexico (Fig. 2) or Ecuador, although applications in bridges in Mexico are common.

Fig. 1 – RCHBs in a bridge in Lisbon, Portugal

Fig. 2 – RCHBs in a building in Mexico City

Despite the common use of RCHBs in bridges and buildings, there are still few experimental research studies for this structural element. Surprisingly as it may seem, most of them have focused to study their shear behavior under static loading [1-4]. Before conducting the research reported herein, there was only one study available for RCHBs failing in shear under a continuity condition [5]. To the authors´ knowledge, the only cyclic testing available for a shear failure are the ones conducted by this research team for simply-supported RCHBs with and without shear reinforcement [6]. Due to the aforementioned, it is not surprising that the design of RCHBs is not addressed in most specialized reinforced concrete textbooks; only few of them include brief sections [i.e., 7]. Although in these books it is considered the contribution of the inclined steel reinforcement in the shear resisting mechanism, which it is correct, this contribution is considered under the assumption that RCHBs develop shear cracking patterns similar to those developed in prismatic beams, which it is not precise based upon experimental evidence [1-6]. Another consequence of having limited experimental information for RCHBs is that there are no specific recommendations for haunched beams in the reinforced concrete guidelines most commonly used in Mexico that would insure a proper shear and flexural design.

Therefore, it seems that the design of RCHBs worldwide has been mostly left to the experience and judgment of structural engineers in professional practice. Taking aside isolated experiences where the shear design of RCHBs have been done using suitable design methods, it seems that most practicing engineers have been forced to extrapolate their knowledge about the static and cyclic behavior of RC prismatic beams to more complex RC non-prismatic beams. Should these extrapolations would be good enough to warrant satisfactory seismic performances of bridges and buildings with RCHBs? The first author witnessed the shear failure of several RCHBs in two midrise buildings at the lakebed zone in Mexico City when participating in reconnaissance teams to document the effects on buildings of the September 19, 1985 Michoacán Earthquake.

Those buildings were severely damaged during the 1985 earthquake and demolished afterwards. Therefore, it seems that, at the times, these extrapolations were not good enough to warrant a satisfactory performance.

In order to insure the desirable ductile behavior of RCHBs according to capacity-design rules, it is necessary first to understand how sudden failures under monotonic and cyclic loads occur, for example, the shear failure. Once this goal is achieved, it can be possible to study how to warrant a ductile flexural failure. Therefore, in this paper the experimental results of RCHBs designed to develop shear failure and tested under cyclic loading under a continuity condition are presented. This study complements previous studies of similar simply-supported RCHBs subjected to static [4] and cyclic [6] loading. For space constraints, only some of the relevant processed results are summarized and discussed in following sections.

2. Description of test specimens

The geometry of prototypes RCHBs was defined according to a survey conducted in existing bridges and buildings in Mexico City (i.e., Fig. 2) and the limitations of our experimental lab. A double-cantilever setup was chosen (Fig. 3), similar to the one used by MacLeod and Houmsi in their smaller-size specimens [5]. The width (b) for all beams was 25 cm, the effective span (L) was 370 cm, and the shear span (a) was 150 cm. The haunched length (L_h) at both beam ends was one-third the effective span (L_h=L/3≈125 cm). Five different linear tapering geometries were obtained by keeping constant the overall depth at each beam end (h_{max}=45 cm) and reducing the overall depth at the central prismatic length to h_{min}=45 (prismatic control element), 38, 31, 27 and 23 cm. Therefore, haunched angles from the horizontal (α) were 0°, 3.21°, 6.39°, 8.19° and 10.43° respectively. The geometry of all prototypes satisfied the requirement L/h>5 to be considered as slender beams by the Mexican code (L/h_{max}>5). In addition, with the purpose of not magnifying the characteristic arching mechanism observed experimentally and analytically in haunched beams [1, 2], all prototypes were checked to fulfill the well-known a/d limiting ratio between slender beams and short beams (a/d_{max}>2.5). The top and bottom reinforcement cover was 5 cm. The specified material properties for design were a compressive strength f'_c=250 kg/cm^2 for the concrete, and a yield tensile stress f_y= 4200 kg/cm^2 for all the steel reinforcement.

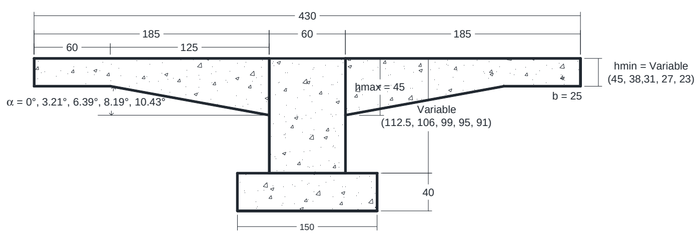

Fig. 3 – Global dimensions of test specimens (units: mm)

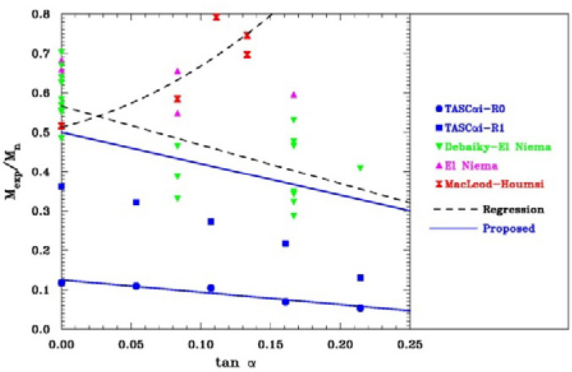

Fig. 4 – Indirect contribution of the inclined longitudinal reinforcement from previous tests

3. Considerations for the design of test specimens

Mörsch [1] presented the pioneering work where he demonstrated analytically that the major difference between simply-supported RCHBs and RCHBs under a continuity condition in resisting shear is due to the contribution of the inclined reinforcement in function of their geometry and loading conditions. For example, consider the cantilever and simply-supported RCHBs under the action of concentrated static load **P** depicted in Fig. 5. For the cantilever haunched beam (Fig. 5a), the bending moment diagram increases in the same direction that the depth of the haunch increases and, under such condition, Mörsh demonstrated that the contribution of the inclined reinforcement (V_{isr}) adds to the nominal shear strength (V_{nHB}). In contrast, for the simply-supported haunched beam (Fig. 5b), the bending moment diagram increases in the opposite direction that depth of the haunch increases, and in such condition, the contribution of the inclined reinforcement (V_{isr}) reduces the nominal shear strength (V_{nHB}). It is worth noting that the positive or negative contribution of the inclined reinforcement to resist the shear force is independent of the supporting condition: it adds if the moment increases in the same direction as the depth increases, and it subtracts when the depth decreases while the moment increases.

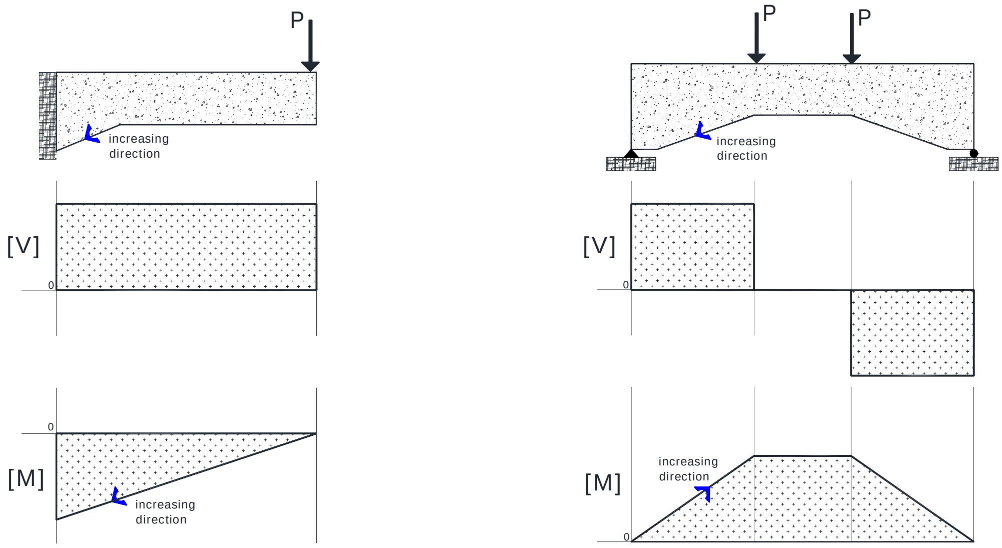

$$V_{nHB} = V_{pc} + V_s + V_{isr}$$

a) Continuity condition

$$V_{nHB} = V_{pc} + V_s - V_{isr}$$

b) Simply-supported condition

Fig. 5 – Shear resistance of RCHBs for the indicated loads and supporting conditions

The theory developed by Mörsch was confirmed using available experimental data from previous tests on RCHBs [3, 4]. For example, in a previous work [4], in order to assess the magnitude of the effective bending moments developed by the tested simply-supported haunched beams (similar geometry and testing conditions as depicted in Fig. 5b), the applied bending moment (M_{exp}) associated to the shear force that caused bond slip, as determined from visual observations and the strain measurements for the longitudinal steel reinforcement at that section, was normalized with respect to the nominal bending moment (M_n) that the same section could developed if the beam could fail in flexure. For this purpose, M_n was computed considering the equivalent stress block proposed by the ACI 318 code [8] and the provided flexural reinforcement, as well as experimental values reported for f'_c and f_y. A similar procedure was conducted using experimental results reported by Debaiky and El-Niema [2] and El-Niema [3] for simply-supported prismatic and haunched beams of similar geometry (Fig. 5b) and for the double-cantilever haunched beams (Fig. 3) tested by MacLeod and Houmsi [5] of similar geometry and loading as the one depicted for the simple cantilever in Fig. 5a. The difference was that the applied bending moment (M_{exp}) computed for those experiments was directly related to the reported shear force at failure, because shear forces that may have caused bonding failures were not reported in these cited works.

The obtained M_{exp}/M_n ratios were plotted versus $\tan\alpha$ as shown in Fig. 4, where α is positive for haunched beams of increased depth at support. In this figure, the results of beams with shear reinforcement are identified as TASCαi-R1, Debaiky–El Niema and El Niema, whereas the results of beams without shear reinforcement are identified as TASCαi-R0 and MacLeod-Houmsi. Many observations can be done from Fig. 4, as discussed in greater detail elsewhere [4]. It was confirmed that under a continuity condition (MacLeod and Houmsi), the contribution of the inclined longitudinal reinforcement adds and tend to increase as the haunch angle α increases. In contrast, for simply-supported beams, the contribution of the inclined longitudinal reinforcement subtracts and tends to decrease as the haunch angle α increases.

Then, test specimens were designed to develop a shear failure [9] using the same principles and procedures of previous tests [4, 6]. To insure a shear failure along the haunches, the design was made providing the flexural capacity at the beam-column joint and in the central prismatic length and keeping continuous the longitudinal reinforcement along the prototypes. All the specimens were designed to insure that they failed in shear with the experience gained from previous work to assess the shear strength of RCHBs [4, 6].

The following considerations were done. Because of the continuity condition of the double-cantilever setup (Fig. 3) and that cyclic loads would be applied similar to what it is illustrated in Fig. 5a, the nominal shear strength (V_{nHB}) for the haunched beams was assessed as:

$$V_{nHB} = V_c + V_s \tag{1}$$

$$V_c = V_{pc} + V_{isr} \tag{2}$$

where V_c is the concrete shear strength that takes into account the contribution of the longitudinal inclined reinforcement, V_{pc} is the nominal concrete shear strength of constant depth beam having the same cross section as that considered for haunched beam, V_{isr} is the shear contribution of the inclined steel reinforcement and V_s is the contribution of the transverse steel reinforcement. In Eq. (1), V_{pc} and V_{isr} terms were obtained from the moment equilibrium equation at the section of interest.

Individual shear contributions were assessed as follows. For consistency with prismatic sections, V_{pc} was derived in terms of the equation proposed by the ACI 318 code [8]:

$$V_{pc} = \left(0.5\sqrt{f'_c} + 176\rho_w \frac{V_n d_{cr}}{M_n}\right) b d_{cr} \tag{3}$$

where f'_c is the nominal compressive strength for the concrete, V_n and M_n are the nominal shear force and bending moment at the critical haunched section (absolute values), ρ_w is the ratio of longitudinal reinforcement, b is the width of the beam and d_{cr} is the effective equivalent depth at the critical haunched section, which is estimated as [4, 6]:

$$d_{cr} = d_{min}\left[1 + 1.35\tan\alpha\right] \leq \left[\left(\frac{h_{max}h_{min} - h_{max}^2}{2l_h} + h_{max}\right) - r\right] \tag{4}$$

where d_{min} is the minimum effective depth for the haunched beam, α is the angle of slope of haunch from horizontal, h_{max} and h_{min} are the maximum and minimum depth of the haunched beam respectively, l_h is the haunched length and r is the concrete cover for the longitudinal reinforcement.

According to what it has been proposed before [4], the contribution of the transverse steel reinforcement is assessed as:

$$V_s = \frac{A_v f_{yv} d_{cr}}{s\tan(45 - \alpha)} \tag{5}$$

where A_v is the area of the transverse shear reinforcement, f_{yv} is the yield stress of the shear reinforcement, s is the separation of the transverse shear reinforcement and d_{cr} and α have been already defined.

The contribution of the inclined longitudinal reinforcement is assessed as:

$$V_{isr} = \pm\frac{M_{cr}}{d_{cr}}\tan\alpha \tag{6}$$

where M_{cr} is the developed bending moment at the critical section accounting premature bond-slip failures of the inclined reinforcement in over-reinforced beams. Taking into account that: a) the only available experimental information for a continuity condition was the one reported by MacLeod and Houmsi (Fig. 4) for RCHBs without shear reinforcement and, b) observing the differences for simply-supported beams with and without shear reinforcement from the available data (Fig. 4); the developed moment at the critical section M_{cr} was preliminary assessed as:

$$M_{cr} = 0.85 M_n (1 + 1.6 \tan\alpha) \leq M_n \tag{7}$$

Of course, the validity of this proposed equation had to be confirmed with the data obtained from specimen testing, as discussed in following sections.

The transverse steel reinforcement along the haunch was placed at spacing close to the maximum allowed by most reinforced concrete codes ($s_{max}=d/2$). Then, as the maximum depth is 45 cm and the haunched length is 125 cm, the separation used for the construction of the specimens was obtained from adjusting the theoretical s_{max} to 25 cm, in order to have stirrups equally spaced and still favoring a shear failure. Additional shear reinforcement nearby the vertex and beam-column interfaces was placed to account for the abrupt change of direction of the bottom longitudinal reinforcement. For this purpose, a recommendation originally proposed by Park and Paulay [7] was adapted, as explained elsewhere [6, 9]. Finally, the shear reinforcement at the prismatic section was very closely spaced (over-confined) to reduce the possibility of having a local failure due to the application of the load. Following the described general design procedure, the provided reinforcement is summarized in Table 1. Typical arrangements are shown in Fig. 6.

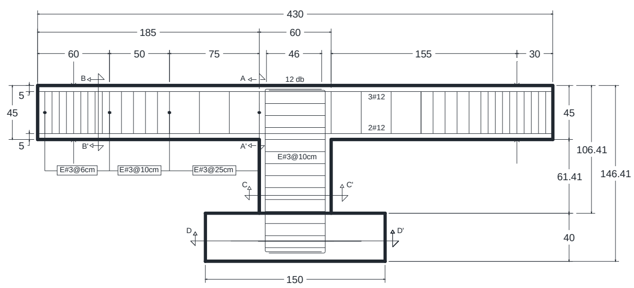

a) TASCV0α0-R1c

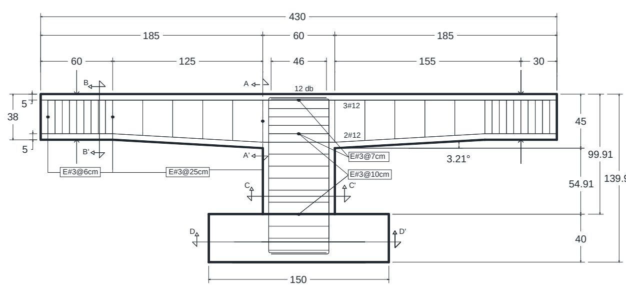

b) TASCV3α1-R1c

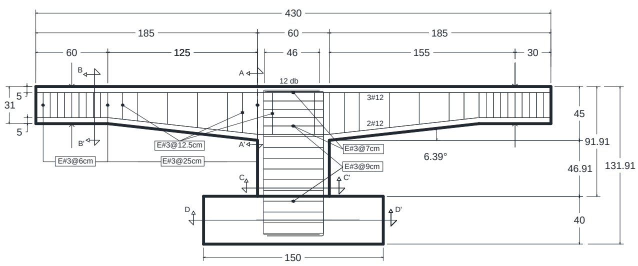

c) TASCV3α2-R1c

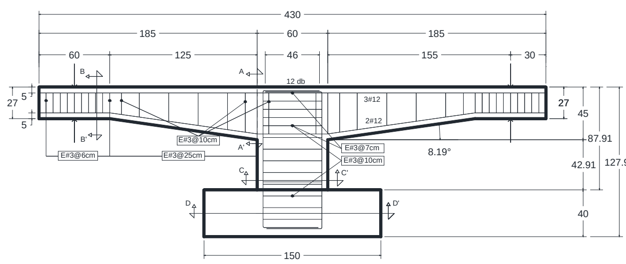

d) TASCV3α3-R1c

Fig. 6 – Reinforcement for beam specimens (dimensions in mm)

Table 1 – Identification of test specimens

Beam ID	α	Flexural Reinforcement		Shear Reinforcement			
		Top	Bottom	Prismatic section	Haunched length	Vertex	Beam-Column Joint
TASCV3α0-R1c	0°	3#12	2#12	9S#3 @ 6 cm	5S#3 @ 10cm 4S#3 @ 25 cm	-	-
TASCV3α1-R1c	3.21°	3#12	2#12	9S#3 @ 6 cm	6S#3 @ 25 cm	-	-
TASCV3α2-R1c	6.39°	3#12	2#12	9S#3 @ 6 cm	6S#3 @ 25 cm	2S#3 @ 12.5cm	2S#3 @ 12.5cm
TASCV3α3-R1c	8.19°	3#12	2#12	9S#3 @ 6 cm	6S#3 @ 25 cm	2S#3 @ 10cm	2S#3 @ 10cm

4. Instrumentation and test displacement history

In order to assess the contribution of the steel reinforcement, beams were internally instrumented with strain gages to measure tensional and compressional strains in the longitudinal steel reinforcement along the haunched length, as well as to measure strains of stirrups in the same zone, as schematically depicted in Fig. 7. Beams were tested under concentrated cyclic loads (V) that were applied 30 cm from the vertex formed by the intersection of tapered sections with the prismatic section towards the end of the prismatic section, as depicted in Fig. 8. Applied loads were measured with load cells at each point of loading. External instrumentation for cyclic loading was designed to measure vertical deflections at mid-haunch, the vertex and the beam-end of the prismatic section, plus two diagonal transducers to measure distress at the column –beam-column joint, and the applied loads with two load cells (Fig. 8).

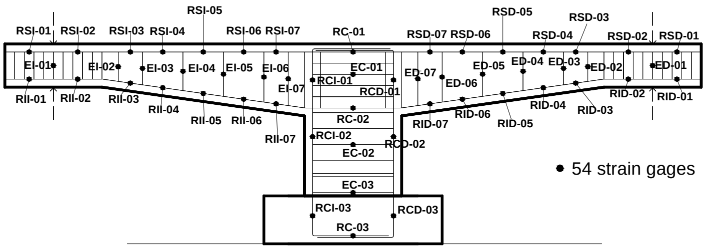

Fig. 7 – Internal instrumentation, specimen TASCV3α3-R1c

Fig. 8 – External instrumentation, TASCV3α3-R1c

Cyclic tests were displacement-controlled in terms of the measured displacement at the vertex, Δ. Vertex displacement increments of 3 mm were set in the displacement history in beams up to 12 mm, and then, displacement increments of 4 mm were used. Negative loads (gravity direction, Fig. 9) induce a negative moment and vice versa. Two cycles at the same displacement were set in the displacement history, as schematically depicted in Fig. 10. This was done in order to evaluate key structural parameters such as stiffness and strength degradation, energy dissipation, equivalent viscous damping, etc. Tests were stopped when beams lost the ability of supporting more load, due to excessive damage (structural instability). Each half-cycle depicted in Fig. 10 has a color code that has a direct relation with the color used to mark the cracks that occurred at that half cycle.

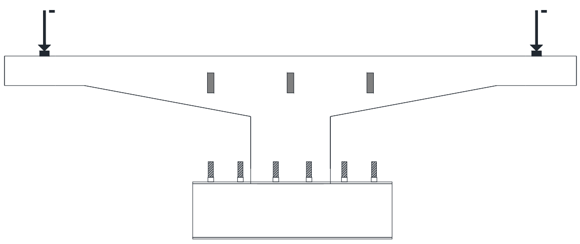

Fig. 9 – Application of cyclic load (M^-)

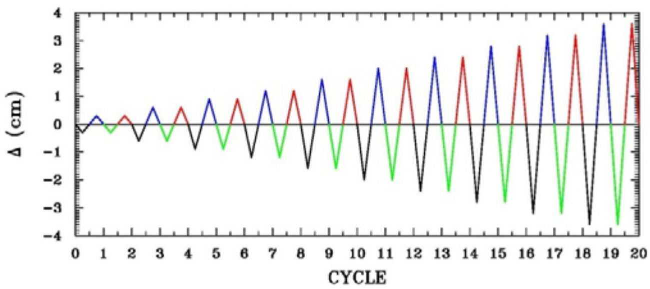

Fig. 10 – Cyclic displacement history

5. Experimental results

Hysteretic curves obtained for the test specimens are depicted in Figure 11. The measured deflection at the vertex was normalized with the haunched length (l_h=125 cm) to obtain the drift angle (Δ) of the haunched beams and shown as percentage in Fig. 11. Shear forces (V) correspond to those measured with load cells at the left and right haunches. It can be observed that stiffness and strength degradations start to be notorious around a drift angle Δ=1.5%. Also, it is confirmed that as expected, because the geometry and reinforcement asymmetry of the prototypes with respect to a longitudinal axis (Fig. 6 and Table 1), resisting shear associated to negative moment is greater than at the positive moment. It is worth noting that for both negative and positive moment, peak resisting shear forces in haunched beams are very similar to those of the prismatic beams, as it can be confirmed in Table 2 (V_u). This is in contrast with previous tests [4, 6], where increasing the haunched angle diminished the shear capacity of the beams because the concrete resistance was adversely affected by the inclined reinforcement (Fig. 5b) and the volume of concrete diminishes as the haunched angle increases.

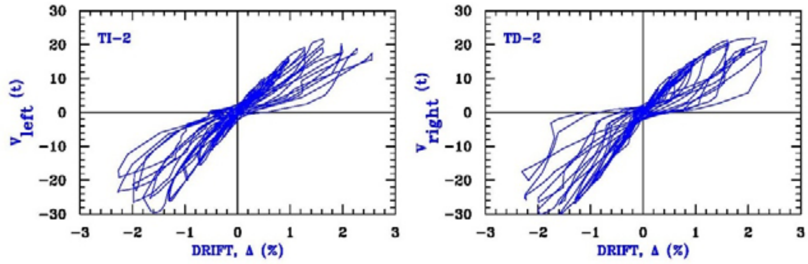

a) TASCV3α0-R1c

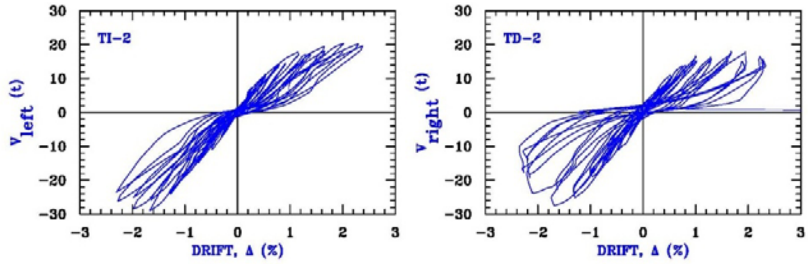

b) TASCV3α1-R1c

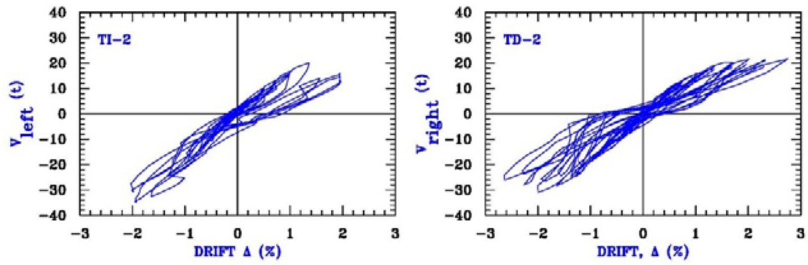

c) TASCV3α2-R1c

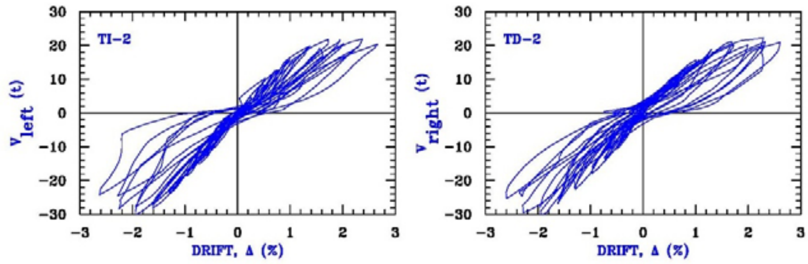

d) TASCV3α3-R1c

Fig. 11 – Hysteretic curves for beams TASCV3αi-R1c

On the basis of experimental observations and in agreement with previous tests [4, 6], three characteristic forces were identified from the full hysteretic response: 1) the shear force that caused the first diagonal cracking (V_{cr}), 2) the ultimate (maximum) shear force (V_u) and, 3) the shear that caused the collapse of the beams (V_{clps}). The characteristic shear forces already described are summarized in Table 2. Finally, the displacements and drifts at the vertex associated to each characteristic stage are summarized in Table 3. For space constraints, only the processed results for the left haunch are reported from now on, as the shear failure generally occurred there.

It can be observed from Table 2 that, except for specimen TASCV3α1-R1c, there are small differences in the three characteristic forces between the prismatic beams and the haunched beams, although the strength decay (difference between V_u and V_{clps}) is in general more pronounced for the prismatic beam. It can also be observed from Table 3 that first cracking generally occurred at a vertex displacement near 6 mm (Δ= 0.5%), except for specimen TASCV3α1-R1c, where it did occur at smaller drifts. In general, haunched beams developed their peak shear force V_u at a relatively larger drift Δ_u than the prismatic beam, particularly at haunched angles greater than 6^0 (specimens TASCV3α2-R1c and TASCV3α3-R1c) and for negative moment.

Table 2 – Measured experimental shear forces from cyclic tests, left beam

Beam ID	V_{cr}^- (t)	V_u^- (t)	V_{clps}^- (t)	V_{cr}^+ (t)	V_u^+ (t)	V_{clps}^+ (t)
TASCV3α0-R1c	11.10	29.49	19.43	10.29	21.63	15.69
TASCV3α1-R1c	6.61	28.90	23.53	7.22	20.40	19.71
TASCV3α2-R1c	10.75	35.06	25.82	10.16	20.07	13.51
TASCV3α3-R1c	10.97	30.49	24.22	10.31	21.95	20.51

Table 3 – Measured experimental displacement (mm) and drifts (%) at the vertex from cyclic tests, left beam

Beam ID	Δ_{cr}^-	Δ_u^-	Δ_{clps}^-	Δ_{cr}^+	Δ_u^+	Δ_{clps}^+
TASCV3α0-R1c	5.98 (0.48%)	19.36 (1.55%)	32.80 (2.62%)	6.46 (0.52%)	20.38 (1.63%)	32.18 (2.57%)
TASCV3α1-R1c	3.58 (0.29%)	20.85 (1.67%)	28.83 (2.31%)	3.30 (0.26%)	25.23 (2.02%)	29.76 (2.38%)
TASCV3α2-R1c	6.06 (0.48%)	24.14 (1.93%)	32.30 (2.58%)	6.22 (0.50%)	16.98 (1.36%)	33.16 (2.65%)
TASCV3α3-R1c	6.28 (0.50%)	24.28 (1.94%)	32.84 (2.63%)	6.58 (0.53%)	29.72 (2.38%)	33.12 (2.65%)

Cracking patterns at the ultimate (peak) shear force V_u are depicted at Fig. 12 for the tested beams. It can be confirmed from the patterns depicted in Fig. 12 that, as in previous tests [4, 6], it is observed that a better cracking distribution is developed in RCHBs compared to the prismatic beam. The observed behavior for RCHBs is less brittle than for the prismatic beam, as the shear failure for RCHBs is noticeably less sudden than the one presented in the prismatic beam.

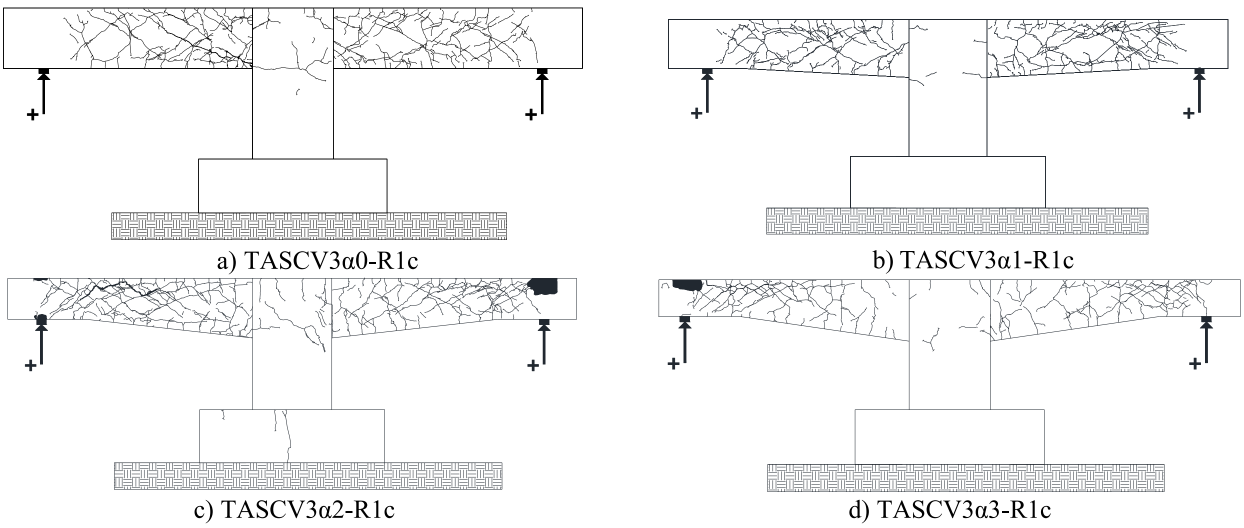

a) TASCV3α0-R1c b) TASCV3α1-R1c
c) TASCV3α2-R1c d) TASCV3α3-R1c

Fig. 12 – Cracking patterns in beams TASCV3α*i*-R1c at ultimate load V_u

In order to assess the magnitude of the effective bending moments developed by the tested haunched beams TASCV3αi-R1c, the maximum developed bending moment (M_{exp}) at the critical section failing in shear (including bond-slip), as determined from visual observations (Fig. 12) and the strain measurements for the longitudinal steel reinforcement at that section, was normalized with respect to the nominal bending moment (M_n) that the same section could developed if the beam could fail in flexure. For this purpose, M_{exp} and M_n were computed considering the unconfined concrete curve proposed by Hognestad [7] and the provided flexural reinforcement (Table 1), projecting the inclined longitudinal reinforcement, as well as experimental values obtained from cylinder tests for f'_c, E_c [9] and considering f_y=4,348 kg/cm^2 for the longitudinal reinforcement. It is worth noting that in the assessment of M_{exp}, the following assumptions were done: (a) the position of the neutral axis and the maximum compressive strain for the concrete (ε_c) were defined based upon strain measurements of the longitudinal reinforcement assuming that plane sections remain plane and, (b) using the curve proposed by Hognestad, equilibrium equations were solved, so in addition to M_{exp}, and effective axial force was obtained (compression or tension). In fact, an effective compression force was obtained in most half cycles before reaching V_u, and an effective tension force was obtained near V_u to V_{clps}. The assessed M_{exp}/M_n ratios were plotted versus $\tan\alpha$ as shown in Fig. 13, where α is positive for haunched beams of increased depth at the beam-column joint. The following is observed from Figure 13: (a) for the same haunched beam, the M_{exp}/M_n ratios are higher for positive moment than for negative moment, as the inclined reinforcement developed higher strains, (b) few M_{exp}/M_n ratios are higher than 1.0 for positive moment, since the maximum moment occurred in flexural compression without bond-slip problems, (c) the proposed Eq. (7) used for the design ("Design") overestimated most of the developed bending moments and, (d) despite of the dispersion obtained for the tested beams, a linear regression is plausible for practical purposes. Therefore, based upon the linear regression of the tested TASCV3αi-R1c beams, in order to improve the estimates of M_{cr} for RCHBs where the moment increases in the same direction as the depth increases, the following equation is proposed (Fig. 13):

$$M_{cr} = 0.75 M_n (1 + \tan\alpha) \le M_n \tag{8}$$

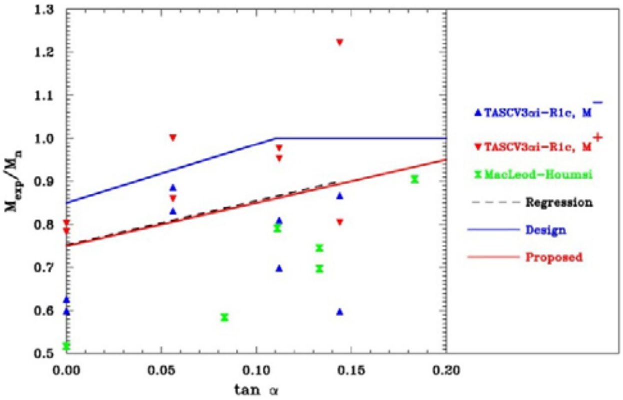

Fig. 13 – Indirect contribution of the inclined longitudinal reinforcement from tests

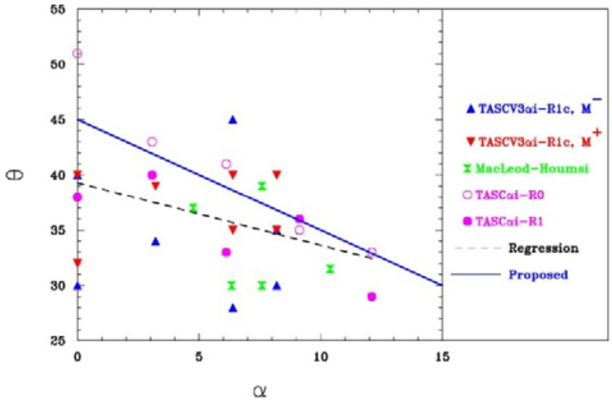

Fig. 14 – Measured angle of inclination of the principal shear crack with respect to an horizontal axis (θ) versus the angle of inclination of the haunch (α)

The angles of inclination of the principal shear crack with respect to an horizontal axis (θ) were measured and added to a previous compiled database [4] and plotted versus α as shown in Fig. 14. As depicted in Fig. 14, a linear regression is still plausible despite the dispersion. For practical purposes and for consistency with the design already established for prismatic sections (assumed angle of inclination for the shear crack of 45^0), the previously proposed equation $\theta = 45 - \alpha$ (Fig. 14) is conservative but valid, so the contribution of the transverse steel reinforcement can be assessed with Eq. (5).

Therefore, in order to assess the effectiveness of the proposed empirical equations obtained from the equilibrium of the critical section, the estimates for V_{nHB} using these expressions (Eqs. 1 to 6 and 8) are compared with the experimental ones (V_{uef}) in Tables 4 and 5, using the experimental values for f'_c at the date for testing reported there. Also, it is worth noting that in order to obtain the effective experimental ultimate shear force, V_{uef}, the applied load V_u was corrected taking into account the shear force due to the assessed self-weight of the beam at the critical section (V_{sw}), as the self-weight adds for negative moment (gravity direction) and subtracts for positive moment. It is worth noting that experimental V_s was assessed adding the forces developed by the stirrups which were crossed by the major shear crack. Individual forces at each stirrups were estimated from their measured strains and assuming and elastic-perfectly plastic behavior for the steel (as peak strains were not high) and using the experimental yield stress f_{yv}=4,592 kg/cm^2 obtained for the shear reinforcement. The experimental V_{isr} was assessed from Eq. (6) and considering that: a) M_{cr}=M_{exp}, assessing M_{exp} as explained before and, b) d_{cr} is the effective depth at the critical shear section. Given that direct measurements for V_c and V_{pc} were not possible, they were indirectly assessed from the most reliable experimental measurements. Therefore, experimental V_c was assessed as V_c=V_{uef}-V_s, whereas experimental V_{pc} was obtained as V_{pc}=V_c-V_{isr} and if a negative value was obtained at the failure stage, a hyphen is shown (Table 5).

Table 4 – Estimates of nominal shear strength of tested RCHBs, left beam, negative bending moment

Beam ID	f´c (kg/cm^2)	From proposed empirical equations					From experimental measurements							V_{nHB}/V_{uef}
		V_{pc} (t)	V_{isr} (t)	V_c (t)	V_s (t)	V_{nHB} (t)	V_{pc} (t)	V_{isr} (t)	V_c (t)	V_s (t)	V_u (t)	V_{sw} (t)	V_{uef} (t)	
TASCV3α0-R1c	292.25	9.47	0.00	9.47	10.43	19.90	17.29	0.00	17.29	12.46	29.49	0.26	29.75	0.669
TASCV3α1-R1c	269.08	8.41	5.04	13.44	10.36	23.80	11.25	5.25	16.50	12.65	28.90	0.25	29.15	0.816
TASCV3α2-R1c	286.48	7.63	9.19	16.81	9.78	26.59	3.49	12.21	15.71	19.56	35.06	0.21	35.27	0.754
TASCV3α3-R1c	255.47	6.60	10.98	17.59	9.16	26.75	2.09	9.23	11.33	19.41	30.49	0.25	30.74	0.870

Table 5 – Estimates of nominal shear strength of tested RCHBs, left beam, positive bending moment

Beam ID	f´c (kg/cm^2)	From proposed empirical equations					From experimental measurements							V_{nHB}/V_{uef}
		V_{pc} (t)	V_{isr} (t)	V_c (t)	V_s (t)	V_{nHB} (t)	V_{pc} (t)	V_{isr} (t)	V_c (t)	V_s (t)	V_u (t)	V_{sw} (t)	V_{uef} (t)	
TASCV3α0-R1c	292.25	9.45	0.00	9.45	10.43	19.88	3.95	0.00	3.95	17.42	21.63	0.26	21.37	0.930
TASCV3α1-R1c	269.08	8.30	3.46	11.75	10.36	22.11	-	4.12	2.45	17.71	20.40	0.25	20.16	1.097
TASCV3α2-R1c	286.48	7.44	6.34	13.78	9.78	23.56	-	9.86	6.44	13.36	20.07	0.27	19.80	1.190
TASCV3α3-R1c	255.47	6.37	7.65	14.02	9.16	23.18	-	9.60	2.67	19.08	21.95	0.19	21.75	1.066

From the information reported in Tables 4 and 5, the following relevant observations can be done: a) overall, the assessment of the nominal shear strength for the tested RCHBs using the proposed empirical equation (V_{nHB}) is good enough and conservative for negative bending moment (Table 4); the worse correlation was obtained for the prismatic beam (where the proposed empirical formulation coincides with what it is currently proposed in ACI 318 code), b) overall, the assessment of V_{nHB} for the tested RCHBs is good but somewhat non-conservative for positive moment (Table 5), c) the assessment of V_{isr} from empirical equations is very reasonable compared to experimental ones, particularly for negative moment (Table 4). For positive moment, the assessment of V_{isr} is conservative, as larger forces were estimated experimentally (Table 5), d) for positive moment, the peak shear force was reached at a state where the concrete nearby the top longitudinal reinforcement was almost completely cracked and the critical cross section in tension, so that it is why there are no V_{pc} contributions. All the contribution for the concrete (V_c) is due to the inclined steel reinforcement (V_{isr}), sometimes in excess of what it is required for theoretical equilibrium, e) for negative moment, the peak shear force was reached at a state where the concrete nearby the inclined longitudinal reinforcement was healthy enough so the critical cross section was in compression. However, V_{pc} values obtained from experimental results lead one to conclude that the concrete contribution at failure is reduced as the angle of inclination of the haunch increases, which it makes sense as in agreement with the proposed empirical formulation, f) in general, the contribution of the shear reinforcement (V_s) is considerable underestimated using the empirical formulas with respect to the ones obtained from test results. There is a good reason for this conservative estimation of V_s. As mentioned before, the proposed angle of inclination of the principal shear crack with respect to an horizontal axis (θ) is conservative in nature with respect to experimental data (Fig. 14) in order to keep all the proposed design equations in agreement with the design of prismatic RC beams proposed by ACI-318 code (when α=0). It can be observed from the linear regression of the available data (still scarce) that the average shear angle for a prismatic beam was around θ=39^0. A closer approximation would have been obtained for most beams using a practical equation closer to the linear regression of the available data: $\theta = 39 - 0.6\alpha$. A much closer approximation would have been obtained assuming a practical but non-conservative equation $\theta = 39 - \alpha$. Given that no more experimental data is available about measured shear angles θ for haunched beams failing in shear, the next experimental improvement would be to retrieve an experimental database of θ for prismatic beams as large as possible to define statistically the shear angle for prismatic beams (θ_0), in order to improve the estimate for haunched beams with a expression of the form: $\theta = \theta_0 - \alpha$. However, the most difficult task would not be to found, retrieve or process such experimental data, but to convince reinforced concrete code committee members worldwide to propose in RC codes that the shear angle is $\theta \neq 45^0$ for the design of the shear reinforcement of prismatic members using the critical section method (although they already know this fact!).

6. Concluding remarks

The research results and interpretations of the testing of four prototype continuous reinforced concrete beams (three haunched and one prismatic) designed to develop a shear failure under cyclic loading were presented in this paper. Subject beams were tested with minimum shear reinforcement. Previously proposed empirical design equations were updated and examined, and it was confirmed that for design purposes these equations allows to reasonably assessing their shear strength. Because of space constraints it was not possible to present and discuss within this paper detailed results related to: a) deformation capacity, b) cyclic degradation, c) stiffness degradation and, d) energy dissipation. However, the obtained results from the cyclic testing in continuity conditions [9] allow one to corroborate what it was observed in previous testing for simply supported beams: reinforced concrete haunched beams are more efficient than reinforced concrete prismatic beams, even when they fail in shear. Experimental results also allow one to conclude and recommend that, in order to be efficient, the geometry of haunched beams should follow the design bending moment diagram; that is, the depth of the haunch should increases in the same direction as the bending moment increases. Such RCHBs are more efficient in resisting shear forces, as the inclined longitudinal reinforcement contributes to resist shear forces. Also, such RCHBs are much more efficient in bending, as the plasticity is spread in a larger region along the haunch rather than in a localized plastic hinge are near the beam ends, as it happen in prismatic sections.

7. Acknowledgements

Financial support of Conacyt (Basic Science Project 79878) and Universidad Autónoma Metropolitana are gratefully acknowledged. The construction of test specimens was possible because of the enthusiastic collaboration of several students who unfortunately we cannot acknowledge personally this time.

8. References

[1] Mörsch, E (1952): *Teoría y práctica del hormigón armado, tomo II*. Gili, Argentina.

[2] Debaiky SY, El-Niema EI (1982): Behavior and strength of reinforced concrete haunched beams in shear. *ACI Journal*, **79** (3), 184-194.

[3] El-Niema EI (1988): Investigation of concrete haunched beams under shear. *ASCE Structural Journal*, **114** (4), 917-930.

[4] Tena-Colunga A, Archundia-Aranda HI, González-Cuevas OM (2008): Behavior of reinforced concrete haunched beams subjected to static shear loading. *Engineering Structures*, **30** (2), 478-492.

[5] MacLeod, IA, Houmsi A (1994): Shear strength of haunched beams without shear reinforcement. *ACI Structural Journal*, **91** (1), 79-89.

[6] Archundia-Aranda HI, Tena-Colunga A, Grande-Vega A (2013): Behavior of reinforced concrete haunched beams subjected to cyclic shear. *Engineering Structures*, **49**, 27-42.

[7] Park R, Paulay T (1997): *Estructuras de concreto reforzado*. Limusa, first edition.

[8] ACI-318-14 (2014): Building code requirements for structural concrete (ACI-318-14) and commentary (ACI 318R-14). *American Concrete Institute*, Farmington Hills, Michigan, USA.

[9] Urbina LA (2013): Comportamiento a cortante de trabes acarteladas continuas de concreto reforzado sujetas a cargas cíclicas. *Tesis de Maestría*, Posgrado en Ingeniería Estructural, División de Ciencias Básicas e Ingeniería, Universidad Autónoma Metropolitana Azcapotzalco, diciembre.